8-2

2D Analytical Model for the Study of NEM Relay Device Scaling

Xiaoying Shen, Soogine Chong, Daesung Lee, Roozbeh Parsa, Roger T. Howe, H.-S. Philip Wong
Department of Electrical Engineering
Stanford University, CA 94305
{xyshen, hspwong}@stanford.edu

Abstract – NEM relay is a promising class of device to overcome the power crisis of CMOS circuits. To design these devices and predict their scaling properties, an analytical model highlighting the fundamental physics of the relay operation is highly desired. This work presents a new 2D analytical model for the study of NEM relay scaling. The model retains the physical insights for NEM relays and yet has the simplicity close to the commonly used 1D model. The error as compared to a finite element model is reduced from ~25% (1D model) to ~3% (this work) by introducing a ratio R(α) to account for 2D effects in the 1D formulation. Besides the fundamental mechanical and electrical properties, the model also takes into account surface forces in the operation of NEM relay devices. The impact of surface forces on the operation voltage as devices are scaled down is discussed.

Keywords - nano-electro-mechanical (NEM) relay , two-dimensional analytical model, scaling , MEMS

I. INTRODUCTION

Transistor leakage sets a well-defined limit on the energy efficiency of CMOS circuits independent of their level of parallelism [1]. The nano-electro-mechanical (NEM) relay promises to overcome this roadblock for they feature zero leakage and infinite subthreshold slope (Fig. 1) NEM relay-based adders have been demonstrated to achieve >10× energy efficiency gain over optimized CMOS adders [2].

In this paper, we consider the 3-terminal (3T) NEM relay as a prototypical NEM relay device. A conventional 3T NEM relay consists of a cantilever beam (or the source electrode) separated from the gate electrode by an air gap of g_0 (Fig. 2) and from the drain electrode by an air gap smaller than g_0 (not shown in Fig. 2) so that, upon actuation, the beam makes contact to the drain and not to the gate. The attractive force between the beam and the gate that deforms the cantilever beam is dominated by the electrostatic force F_{ele} at a g_0 larger than a critical dimension, g_{c0} (The value of g_{c0} depends on design variables of device dimensions). For devices with g_0 smaller than g_{c0}, the influence from surface attractive forces, such as van der Waals force (F_{vdw}), becomes more significant and loads the beam together with the electrostatic force [3]. When the beam pulls towards the gate, a balance is established between the restoring elastic force (F_{ela}) from beam deformation and the attractive forces ($F_{attractive}$, e.g. F_{ele}). As the beam deforms, $F_{attractive}$ increases faster than F_{ela}, and at a critical pull-in voltage (V_{pi}), F_{ela} can no longer balance $F_{attractive}$. The beam becomes unstable and collapses towards the gate electrode, making contact to the drain electrode. The status of beam right before pull-in ("Pull-in Point") is critical. The pull-out voltage (V_{po}), another critical voltage in relay operation, is the minimum voltage needed to hold the beam at the pull-in state and is less than or equal to V_{pi} (Fig. 1). V_{pi} and V_{po} are important properties, determining the delay and power of NEM relay operations. With carefully designed device dimensions, the hysteresis window between V_{pi} and V_{po} can be made sufficiently narrow [3]. Therefore, we focus our discussion of operation voltage on V_{pi} as it sets a minimum boundary for the required power supply voltage.

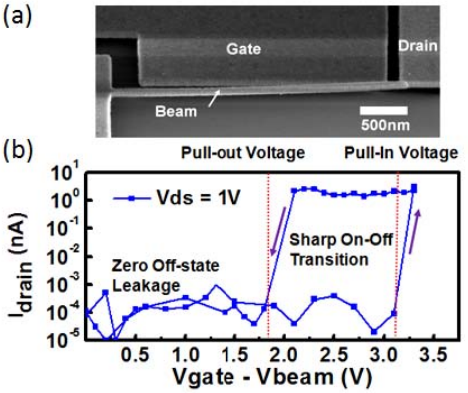

Figure 1 (a) Scanning electron microscope (SEM) image of a laterally actuated 3T NEM relay. (b) I_D-V_{GB} characteristic of the NEM relay in (a), showing desirable properties for low power application: (1) off-state current in noise level; (2) sharp on/off transition. The drain current is limited by a compliance current of 1nA in the measurement.

The existing quantitative study of electrostatically actuated cantilever beams usually requires numerical analysis using iterative calculation methods. There are three widely used analytical models for the pull-in voltage: 1) 1D model with parallel plate assumption [4], 2) linear superposition model (LSM) [5], and 3) planar theory model (PTM) [6]. The error of the 1D model V_{pi} compared to the numerical results is large (~25%) because F_{ele} is over-estimated in the 1D model when calculated from the maximum deflection point on the beam. Both LSM and PTM obtain very similar results with ~1% error compared with numerical results because they take into account the distributed load along the beam. However, LSM can avoid numerical integration only if a square-law curvature beam configuration is assumed, and the boundary-conditions in the PTM need to be solved by iterative methods [5, 6]. When forces other than F_{ele} and F_{ela} (i.e. surface attractive force at the van der Waals (F_{vdw})/Casimir (F_{cas}) regimes [7]) are introduced into the analysis, the square-law assumption in LSM is no longer valid. The numerical step in LSM and iterative calculation in PTM make them difficult to arrive at a solution analytically. Since the surface attractive force is important for assessing NEM relay scaling [3], LSM and PTM are not suitable for simple scaled NEM relay device modeling.

978-1-61284-418-3/11/$26.00 © 2011 IEEE

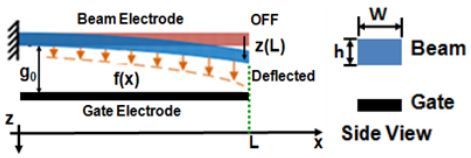

Figure 2 Schematic of the 2D beam deflection model. Beam length L, beam to gate gap size g_0, maximum beam deflection z(L) (z(L) = g_0 at Pull-in Point), and other device parameters are defined as illustrated. f(x) (can be $f_{ele}(x)$, $f_{vdw}(x)$ or $f_{cas}(x)$ under different conditions) is the force per unit length the beam experiences from the actuating gate electrode and varies along the length of the beam. Beam width in direction of movement is defined as *h*, and the beam thickness perpendicular to the direction of movement is W.

II. Model Derivation

The iterative calculations in obtaining V_{pi} come from the coupling of mechanical and electrical behaviors. The beam bending configuration depends on the applied load (i.e. F_{ele}, F_{vdw}) which changes with the distance between the beam and gate electrodes at a certain position, or the beam configuration. Numerical integration, another factor that makes it difficult to obtain an analytical equation for V_{pi}, comes from the integral of various distributed loads (i.e. F_{ele}, F_{vdw}) as a function of the deflection z. Therefore, in order to achieve an analytical equation for V_{pi}, we need to make a reasonable assumption for the beam configuration at Pull-in Point to avoid iterative calculations and an approximation to the integral of the distributed loads along the beam.

The derivation of the 2D model is summarized in Fig. 3. To calculate the restoring force, F_{ela}, we first assume a uniformly distributed load along the cantilever which pulls the beam to the Pull-in Point. With the uniformly distributed load, the beam deflection z(x) can be calculated by solving the Euler-Bernoulli beam equation with boundary conditions for the clamped-free cantilever [8]. The beam configuration can be obtained with

$$z(x) = \frac{q}{24EI}x^2(x^2 - 4Lx + 6L^2) \quad (1)$$

where z(x) indicates the distance between the beam and gate electrodes at position x along the beam. The z(x) calculated from the uniformly distributed load has a fourth-order polynomial dependency on x. The non-uniformly distributed load will show a polynomial dependency higher than fourth-order [9]. The error introduced by the uniformly distributed load assumption is sufficiently small, which is verified by comparing the approximated beam configuration with COMSOL [10] simulated beam configuration. The expression is valid only before Pull-in Point, at which the boundary conditions no longer apply. At the Pull-in Point, x=L, eq. 1 becomes

$$z(L) = \frac{qL^4}{8EI} \equiv \alpha g_0 \quad (2)$$

where αg_0 is maximum deflection at Pull-in Point (Fig. 2). α indicates the ratio between z(L) and g_0 .

At the Pull-in Point, equivalent F_{ela}, which balances the uniformly distributed load and keeps the beam stable, can be represented as

$$F_{ela} = qL = k\alpha g_0 \quad (3)$$

where k is defined as an equivalent spring constant, which can be expressed as

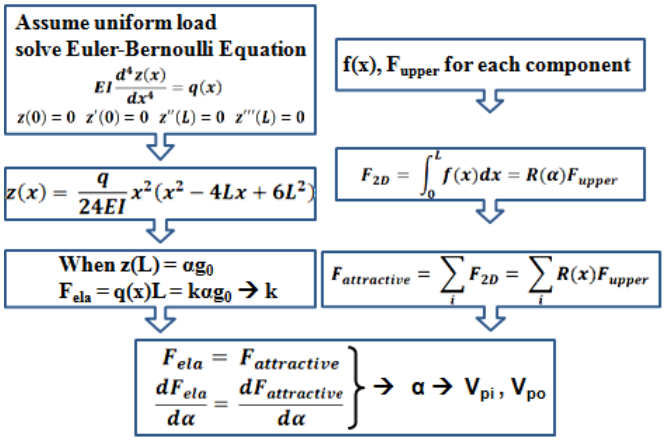

Figure 3 Derivation of the 2D analytical model. Restoring forces (F_{ela}) and attractive forces ($F_{attractive}$) are decoupled. F_{ela} is calculated from the equivalent spring constant. Integration of $F_{attractive}$ is avoided by introducing the ratio factor R(α). E is Young's Modulus of the beam (160GPa for poly-silicon), and I is second moment of area.

$$k = \frac{2}{3}\frac{Ewh^3}{L^3} \quad (4)$$

$F_{attractive}$ on the beam includes different components (neglecting other non-ideal surface adhesion or stiction forces) under different conditions:

1. When g_0 is large (on the order of micrometers), the surface attraction is much smaller than the electrostatic force.

$$F_{attractive} \sim F_{ele} \quad (5\text{-a})$$

2. As g_0 becomes smaller, the surface attraction increases faster than the electrostatic force and becomes increasingly significant. When g_0 is larger than tens of nanometers, the dispersion force is in the Casimir regime [7].

$$F_{attractive} \sim F_{ele} + F_{cas} \quad (5\text{-b})$$

3. When g_0 smaller than the order of several tens of nanometers, the surface attraction is in the van der Waals force regime [7, 11].

$$F_{attractive} \sim F_{ele} + F_{vdw} \quad (5\text{-c})$$

As in the 2D model, we integrate the force per unit length along the beam and get the total attractive force. The force per unit length for each force components, f_{ele}, f_{vdw} and f_{cas}, can be expressed as eq. (6) shown in Table 1. f_{ele} is the derivative of the electrostatic energy stored in the gap capacitor, $CV^2/2$, with respect to the gap size at position x. The fringing effect is neglected. f_{vdw} and f_{cas} come from the definitions [6, 7]. Different forces show different dependencies on the distance between beam and gate ($g_0 - z(x)$). Considering that the expression for z(x) is a fourth-order polynomial equation, the integrations of f_{ele}, f_{vdw} and f_{cas} are very difficult without numerical computation. We need a reasonable approximation to eliminate the integration while maintaining the 2D effects for different forces. As we compare the integral of eq. 7, $F_{2D} = \int_0^L f(x)dx$ and eq. 8, which shows the upper bound for these three forces (see Table 1) calculated from the 1D model (F_{upper}), it is interesting to note that the ratios between F_{2D} and F_{upper} are independent of the applied voltage and device dimensions when the expression of force per unit length has the form

$$f(x) = \text{constant}/(g_0 - z(x))^n \quad (6)$$

Table. 1 Force per length *f*, upper bound F_{upper} and ratio factor $R(\alpha)$ for different force components

	Force per Length *f*(x)	Upper Bound F_{upper}	$R(\alpha) = F_{2D} / F_{upper}$
F_{ele}	$f_{ele}(x) = \frac{\varepsilon_0 W V^2}{2(g_0 - z(x))^2}$ (7-a)	$F_{ele,upper} = \frac{\varepsilon_0 W L V^2}{2(g_0 - z(L))^2}$ (8-a)	$R_{ele} = 1 - 1.2\alpha + 0.2\alpha^2$ (9-a)
F_{vdw}	$f_{vdw}(x) = \frac{A_h W}{6\pi(g_0 - z(x))^3}$ (7-b)	$F_{vdw,upper} = \frac{A_h W L}{6\pi(g_0 - z(L))^3}$ (8-b)	$R_{vdw} = 1 - 1.72\alpha + 0.74\alpha^2$ (9-b)
F_{cas}	$f_{cas}(x) = \frac{\hbar c \pi^2 \eta W}{240(g_0 - z(x))^4}$ (7-c)	$F_{cas,upper} = \frac{\hbar c \pi^2 \eta W L}{240(g_0 - z(L))^4}$ (8-c)	$R_{cas} = 1 - 2.05\alpha + 1.13\alpha^2$ (9-c)

Note: ε_0 = Dielectric constant of air; A_h = Hamaker constant [9]; ħ= reduced Plank's constant (*h*/2); c = speed of light; η=1 for metal-to-metal plates [5]; *h, W, L* are device dimensions (Fig. 2).

If we define the ratio R as

$$R = F_{2D} / F_{upper} \quad (10)$$

then the value of R only depends on α, and n is defined in eq.6. With a second-order polynomial approximation, R for different forces can be expressed as eq. 9 (Table 1, comparison with numerical simulation shown in Fig. 4) and the integration can be well represented by $F_{2D} = R(\alpha) F_{upper}$ (eq. 10). The total attractive force can be represented as

$$F_{attractive} = \sum_i F_{i,2D} = \sum_i R_i(\alpha) F_{upper} \quad (11)$$

As Fig. 3 shows, both F_{ela} and $F_{attractive}$ are now analytically expressed by the device dimensions, material properties, applied voltage, and α. The pull-in voltage can be analyzed in a similar approach as is done in a 1D model.

With eq. 3 and eq. 11 plugged into the equation for the critical voltage for the pull-in condition,

$$F_{ela} = F_{attractive} \quad (12\text{-a})$$

$$\frac{dF_{ela}}{d\alpha} = \frac{dF_{attractive}}{d\alpha} \quad (12\text{-b})$$

According to different components in $F_{attractive}$, α for pull-in beam position can be deduced from the force equilibrium (eq. 12-a) and the derivative respect to α (eq. 12-b). The analytical equation for pull-in voltage in Fig. 5 can be deduced:

$$V_{pi} = \sqrt{\frac{2kg_0^3\alpha(1-\alpha)^2}{\varepsilon_0 WL(1-1.2\alpha+0.2\alpha^2)}} (\alpha = 0.52) \quad (13)$$

III. RESULTS

The results from the 2D analytical model are compared with COMSOL numerical results (Fig. 5-6), mainly focusing on F_{ela}, F_{ele}, and F_{vdw} (since in Casimir regime, the F_{ele} is dominate). The numerical results are verified with experimental data for devices at large dimension. For the devices with $g_0 > g_{c0}$ ($F_{vdw} << F_{ele}$) only F_{ele} is taken into account for $F_{attractive}$. The computed α is ~0.5, which is very close to the numerical result α = 0.47 [5]. The error between calculated V_{pi} and simulation results stays within ~3% (Fig. 5). For the devices with a small enough g_0, pull-in can occur even without an applied voltage due to the F_{vdw} ($F_{attractive} = F_{vdw}$). α calculated for this condition is ~0.4 whereas the numerical result α = 0.36 [5]. Comparing with COMSOL simulation results, for scaled NEM relays where $F_{attractive} = F_{ele} + F_{vdw}$, the error in V_{pi} is ~10% (Fig. 6).

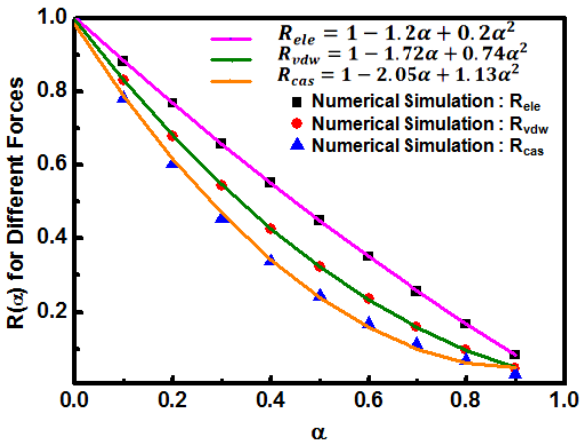

Figure 4 The second-order polynomial approximation (curve) for R(α) verified with numerically calculated results (symbol).

IV. CONSTANT SENSITIVITY SCALING

Similar to MOSFETs, NEM relay devices would demonstrate better performance in terms of delay and power when scaled down to small feature dimensions. Constant-field-scaling (CFS), which scales all the dimensions (g_0, h, W, L) as what we did for MOSFETs, is a possible scaling strategy [12]. However, due to the existence of surface attractive force, CFS turns out not to be the optimal strategy. It is noticed that, if surface attractive force were not present, it would be possible to scale g_0 down to arbitrarily small values (as long as field-emission current between the beam and the drain electrodes is not significant), resulting in a device with shorter operation delay and lower power consumption. However, the surface attractive force increases dramatically when the feature dimension reduces. When g_0 reduces to a dimension small

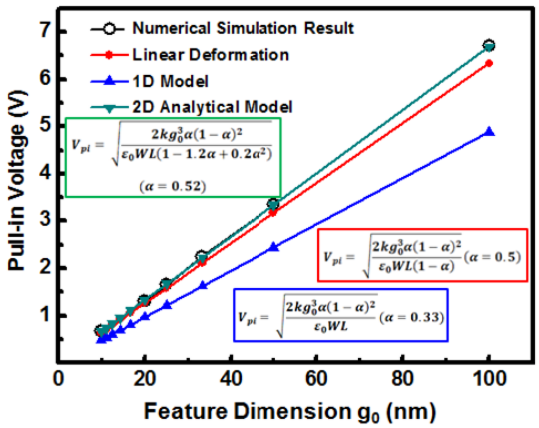

Figure 5 (a) Comparison between 1D model and 2D model for V_{pi} without including F_{vdw}. The error of the 1D model is ~25%. Our 2D model reduces the error to ~3% for V_{pi}.

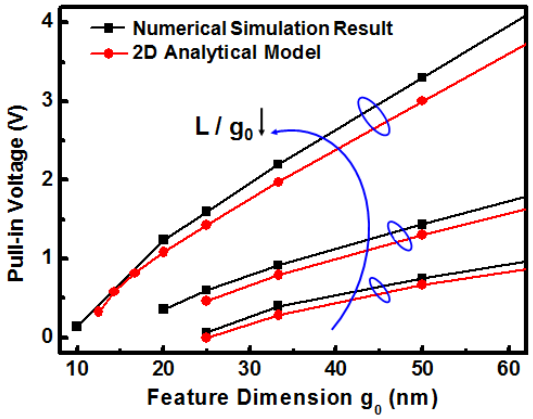

Figure 6 Comparison between 2D model (this work) and numerical simulation for V_{pi} including F_{vdw}. The error is ~10%.

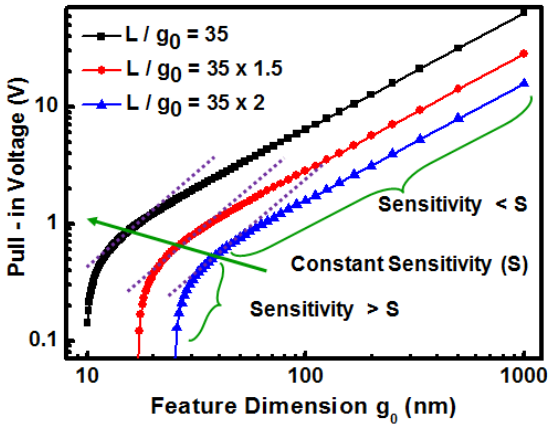

Figure 7 The 2D model can be used for studying the Constant Sensitivity Scaling (CSS) strategy [3, 12] which accounts for device fabrication variation and takes both F_{ele} and F_{vdw} into consideration (see [3] for CSS). Each design curve on plot has a different design choice in L/g_0, follow the arrow to move from one design curve to another, L scales faster than other dimensions to keep S constant.

enough (depends on the other design variables), even without any voltage applied between beam and gate electrodes, the surface attractive force would pull in the beam and hold it at the pull-in state. A better scaling strategy would be Constant-Sensitivity-Scaling (CSS) [3, 12], where sensitivity is defined as

$$S = \frac{d\log V_{pi}}{d\log(g_0)} = g_0 \frac{d\ln(V_{pi})}{dg_0} \qquad (14)$$

S represents the variation in V_{pi} that results from the variation in g_0, which is usually determined by the fabrication process. In CSS, S needs to be smaller than a maximum value which makes sure the devices function properly. When S starts to increase with reduced g_0, the aspect ratio L/h of the beam (which is kept constant in CFS) needs to be reduced to keep S smaller than the maximum acceptable value.

The new model provides a prediction for the critical dimension g_{c0} at which V_{pi} starts to be influenced by F_{vdw} and the slope of V_{pi} vs g_0 at dimensions smaller than this g_{c0} (Fig. 6). Fig. 7 demonstrates different trends for V_{pi} in scaled relay designs, S is calculated from the slope of the V_{pi} vs g_0. When $g_0 > g_{c0}$, V_{pi} reduces linearly in log scale and S keeps constant, thus relay can scale with CFS strategy (stays on one design curve in plot). When $g_0 < g_{c0}$, S is no longer constant and increases with reduced g_0, so S needs to be taken into design consideration. To achieve an immune to variation in g_0, relays must scale with a CSS strategy (move from one design curve to another in plot) by reducing L/g_0.

V. Conclusion

This work proposes a 2D analytical model for NEM relay design which provides a relatively accurate analysis while keeping the simplicity of an analytical solution even when F_{vdw}, F_{cas} are considered. The error between the analytical solutions and 2D simulation results from COMSOL is around 3% when only F_{ele} and F_{ela} are considered for devices with large g_0. The error is ~10% for devices scaled to small g_0 when the impact of F_{vdw} also needs to be considered. The application of newly developed model in CSS is demonstrated and the impact of surface attractive force is discussed. The new model can help designers gain better insights into the balance and competition among the forces at different device dimensions.

VI. Acknowledgment

This work is supported in part by DARPA NEMS, the National Science Foundation, and Center for Energy Efficient Electronics Science (E3S), an NSF funded Science and Technology Center.

VII. Reference

[1] B. H. Calhoun, A. Wang, and A. Chandrakasan, "Modeling and sizing for minimum energy operation in subthreshold circuits", IEEE J. Solid-State Circuits, vol. 40, no. 9, pp. 1778–1786, Sep. 2005.

[2] H. Kam, T. J. King-Liu, V. Stojanovic, D. Markovic, E. Alon, "Design, optimization, and scaling of MEM relays for ultra-low-power digital logic", IEEE TED vol. 58, no. 1, pp. 236-250, Jan. 2011.

[3] K. Akarvardar, H.-S. P. Wong, "Nanoelectromechanical Logic and Memory Devices", ECS Trans., 19(1): 49-59 (2009)

[4] P. M. Osterberg, "Electrostatically actuated microelectromechanical test structures for material property measurements", Ph. D. dissertation, MIT, Cambridge, MA (1995)

[5] R.W. Johnstone and M. Parameswaran, "Theoretical limits on the freestanding length of cantilevers produced by surface micromachining echnology", J. Micromech. Microeng., 12: 855-861 (2002)

[6] A. Ramezani, A. Alasty and J. Akbari, "Influence of van der waals force on the pull-in parameters of cantilever type nanoscale electrostatic actuators", Microsyst. Technol., 12:1153-1161 (2006)

[7] G. I. Klimchitskaya, V. M. Mostepanenko, "Experiment and theory in the Casimir effect," Contemporary Physics, 47(3), pp. 131 - 144, 2006.

[8] S. Gorthi, A. Mohanty, A. Chatterjee, "Cantilever beam electrostatic MEMS actuators beyond pull-in", J. Micromech. Microeng., 16: 1800-1810 (2006)

[9] H. F. Dadgour, M. M. Hussain, C. Smith and K. Banerjee, "Design and Analysis of Compact Ultra Energy-Efficient Logic Gates Using Laterally-Actuated Double-Electrode NEMS", Design Automation Conference (DAC), 2010, Anaheim, CA, 13-18 June 2010.

[10] *COMSOL* Multiphysics®, © 1998-2011 COMSOL.

[11] R. Maboudian and R. T. Howe, "Critical review: adhesion in surface micromechanicstructures," J. Vac. Sci. Technol. B, 15(1), pp. 1-20, 1997.

[12] K. Akarvardar, D. Elata, R. Parsa, G. C. Wan, K. Yoo, J. Provine, P. Peumans, R. T. Howe, H.-S. P. Wong, "Design Considerations for Complementary Nanoelectromechanical Logic Gates," IEEE International Electron Devices Meeting (IEDM), pp. 299-302, 2007.